



# HHS Public Access

Author manuscript

*Colloids Surf B Biointerfaces*. Author manuscript; available in PMC 2015 November 27.

Published in final edited form as:

*Colloids Surf B Biointerfaces*. 2013 December 1; 112: 108–112. doi:10.1016/j.colsurfb.2013.07.045.

## Coating barium titanate nanoparticles with polyethylenimine improves cellular uptake and allows for coupled imaging and gene delivery

Christopher Dempsey<sup>1</sup>, Isac Lee<sup>2</sup>, Katie Cowan<sup>2</sup>, and Junghae Suh<sup>1,\*</sup>

<sup>1</sup>Rice University, George R. Brown School of Engineering, Department of Bioengineering, Houston, Texas

<sup>2</sup>University of Texas at Austin, Cockrell School of Engineering, Department of Biomedical Engineering, Austin, Texas

### Abstract

Barium titanate nanoparticles (BT NP) belong to a class of second harmonic generating (SHG) nanoprobe that have recently demonstrated promise in biological imaging. Unfortunately, BT NPs display low cellular uptake efficiencies, which may be a problem if cellular internalization is desired or required for a particular application. To overcome this issue, while concomitantly developing a particle platform that can also deliver nucleic acids into cells, we coated the BT NPs with the cationic polymer polyethylenimine (PEI) – one of the most effective nonviral gene delivery agents. Coating of BT with PEI yielded complexes with positive zeta potentials and resulted in an 8-fold increase in cellular uptake of the BT NPs. Importantly, we were able to achieve high levels of gene delivery with the BT-PEI/DNA complexes, supporting further efforts to generate BT platforms for coupled imaging and gene therapy.

### Keywords

Polyethylenimine; barium titanate; transfection; second harmonic generation

## 1. Introduction

Inorganic nanoparticles include a vast variety of compounds that exhibit interesting properties at the nanoscale that may not exist in the bulk material. These include various optical characteristics that can be harnessed in biological research to enable the visualization of phenomena at the scale of cells or even subcellular organelles. Barium titanate (BT) nanoparticles (NP) have been known to display unique optical properties since the 1960s [1] but has only recently been used in biological systems [2–3]. Its tetragonal phase is non-centrosymmetric and thus is able to combine two incident photons (of frequency  $\omega$ )

\*Corresponding author, jsuh@rice.edu.

**Publisher's Disclaimer:** This is a PDF file of an unedited manuscript that has been accepted for publication. As a service to our customers we are providing this early version of the manuscript. The manuscript will undergo copyediting, typesetting, and review of the resulting proof before it is published in its final citable form. Please note that during the production process errors may be discovered which could affect the content, and all legal disclaimers that apply to the journal pertain.

emanating from a focused, high-intensity laser into one photon with exactly twice the frequency ( $2\omega$ ) in a process known as second harmonic generation (SHG) [4]. SHG imaging requires a two-photon laser and appropriate filters and can be easily added to a conventional confocal imaging system. Unlike fluorescent probes normally used in confocal microscopy, SHG nanoprobos such as BT do not bleach or blink, can be excited with deeper penetrating long wavelength light, and have a narrow, multi-directional signal spectrum [2]. BT is nontoxic at a range of pHs unlike most quantum dots, which often require surface coatings to protect cells from exposure to their toxic cores [5]. Numerous properties of BT make these nanoprobos promising candidates for biomedical imaging applications.

The BT NPs, however, are inefficient at entering cells without some form of functionalization or conjugation [6] – mainly due to the negative surface charge of the NPs that hinders binding to negatively charged cell surfaces. So far, limited studies have been conducted with BT NPs to improve cellular uptake. In one study, poly-L lysine (PLL) was used to coat BT NPs, resulting in higher cellular uptake [7]. We were interested in building upon this previous work to generate BT NPs not only with positive cellular uptake characteristics, but also with the multi-functional capacity to serve as a coupled imaging and gene delivery agent. PLL is an ineffective transfection agent [8], making it a poor polymer choice when trying to generate nucleic acid-delivering systems. We chose to use polyethylenimine (PEI), a positively charged polymer that has been used frequently as a transfection agent due to its ability to condense negatively charged DNA and deliver it effectively to cells [9]. Additionally, PEI's positive charge allows it to complex with negatively charged NPs, such as BT, while still maintaining its transfection ability [10]. PEI has been used in concert with other polymers due to its ability to enhance uptake into cells and escape endosomes via the hypothesized proton sponge effect [11].

Being able to image the gene delivery vectors allows for researchers to keep track of where the vectors are going during treatments to better understand the ultimate dosage that reaches target cells as well as any unintended destinations. Polymer-stabilized quantum dots have been used for this dual imaging and delivery approach, but the high toxicity of quantum dots makes them poor candidates for extensive *in vivo* studies [12]. Other fluorescent NPs, such as silica-based systems, have also been used in concert with polymers to deliver DNA [13, 14], but conventional fluorescence cannot outperform the narrow signal spectrum and lack of signal saturation that SHG nanoprobos such as BT can offer. Other nanoparticles with contrast enhancing capabilities, such as iron oxide, have been delivered in a nanoparticle-polymer system to deliver DNA in order to obtain simultaneous therapeutic delivery and imaging [15].

Here, we have adsorbed PEI to BT NPs to create complexes with dual imaging and gene delivery capabilities. The BT-PEI does not show significant cytotoxicity and is able to increase the overall uptake into cells compared to uncomplexed BT. DNA transfection studies show that the BT-PEI can deliver genes as effectively as PEI alone. Collectively, our data supports the potential use of BT nanocrystals for simultaneous imaging and delivery of nucleic acids into cells.

## 2. Materials and Methods

### 2.1 Generation and characterization of BT-PEI complexes

Barium Titanate (BaTiO<sub>3</sub>, BT) nanoparticles were purchased from Nanostructured and Amorphous Materials. Particles are of tetragonal configuration and noted by the company to be 200 nm diameter with a purity of 99.9%. Linear 25K molecular weight polyethylenimine (PEI) was purchased from Fisher Scientific.

To form BT-PEI complexes, 500  $\mu$ L of a 1 mg/mL solution of BT was prepared in phosphate buffer (PB, pH 7.4, 10 mM). 500  $\mu$ L of PEI dissolved in PB at varying concentrations was slowly added to the BT solution drop-wise followed by vigorous vortexing for 10 seconds. The solution was then sonicated for 30 minutes (Branson 2510).

Dynamic light scattering (DLS) was performed on a Malvern Zetasizer in low sizing disposable methacrylate cuvettes for size data and in disposable zeta cells for zeta potential measurements. Samples were allowed to equilibrate for 10 seconds before measurements, which were performed at 25 °C. A total of three measurements were taken for each solution for sizing data with the mean of the volume peaks reported.

Thermogravimetric analysis was performed with a Q-600 Simultaneous TGA/DSC (TA Instruments). BT-PEI samples were prepared as above, and centrifuged at 17000 rcf for 10 minutes to sediment particles and washed with 1 mL PB and centrifuged again for 5 minutes. The particles were added to alumina pans and run on the TGA, first heating at 100 °C for 1h and then ramped up to 500 °C at a rate of 2 °C/min [16].

### 2.2 Uptake of BT-PEI complexes into HeLa cells

HeLa cells were cultured in Dulbecco's modified Eagle's Medium (DMEM) that contained 10% fetal bovine serum (FBS) and 1% penicillin streptomycin (P/S) at 37 °C and 5% CO<sub>2</sub>. For uptake studies, cells were plated on poly-L-lysine (PLL) coated coverslips in a 24 well plate for 24 hours after which 70% confluency was achieved. The thickness of cells in a monolayer is estimated to be about 3.6  $\mu$ m [17]. 10  $\mu$ L of 0.5 mg/mL BT or BT-PEI in PB was added to each well and incubated for 3 hours followed by 70% ethanol fixing for 15 minutes and 5 minutes of propidium iodide (PI, 1  $\mu$ g/mL) staining at room temperature. Coverslips were mounted onto slides with fluormount-G and stored at 4 °C overnight before imaging.

A Zeiss 7 laser scanning multiphoton microscope (LSM 7 MP) was used for imaging PI and SHG-producing BT crystals and collected with a non-descanned detector (NDD) through a 40x water objective. Cells were excited with 820 nm light from a 2-photon titanium sapphire laser with a penetration depth of 1000  $\mu$ m [18] and a 390 – 430 nm band pass filter was used for the SHG signal and 500 nm longpass filter for the red PI signal. Particles were counted manually using the ImageJ (NIH) cell counter plugin.

### 2.3 MTT viability assay

HeLa cells were cultured in a 96 well plate overnight until 90% confluency. 10  $\mu$ L of 0.5 mg/mL BT, BT-PEI, and PEI were added to wells (resulting in a final PEI concentration of

2.5  $\mu\text{g/ml}$ ) in duplicate and incubated overnight. Cells were then washed and 100  $\mu\text{L}$  of DMEM (with 10% FBS and 1% P/S) was added to each well. 10  $\mu\text{L}$  of 3-(4,5-dimethylthiazol-2-yl)-2,5-diphenyltetrazolium bromide (MTT), purchased from Invitrogen and diluted to 12 mM in PBS, was added to each well and incubated for 3 hours at 37  $^{\circ}\text{C}$ . A 70% ethanol-killed cell control was used to subtract background signal and wells that had PB added were used as positive controls for 100% viability. All but 25  $\mu\text{L}$  of media was removed from each well and 50  $\mu\text{L}$  of dimethyl sulfoxide (DMSO) was added to each well and incubated for 10 minutes at 37  $^{\circ}\text{C}$ . Sample absorbance was read using a Tecan Magellan plate reader at 540 nm. An average of 16 points of absorbance for each well was used to calculate the absorbance for a given well. Background signal from control wells was subtracted from all other samples and normalized to the PB control.

## 2.4 Transfection assay

HeLa cells were cultured in a 24 well tissue culture plate overnight until 70% confluency. PEI or BT-PEI complexes were used to condense plasmid DNA encoding GFP (pGFP) by adding 25 ng of DNA to varying amounts of PEI or BT-PEI to obtain different N/P ratios [9] followed by immediate vortexing and incubation for 10 minutes at room temperature. Solutions were added to the wells and incubated for 18 hours followed by changing the media and further incubation for another 24 hours. Cells were harvested by first washing with 0.5 mL PBS followed by trypsinizing with 0.2 mL of trypsin and neutralization with 0.2 mL serum complete DMEM. The cells were pelleted and resuspended in 500  $\mu\text{L}$  PBS with 5 mM EDTA and added to a tube through a cell strainer to separate any cell aggregates. Flow cytometry was performed with a BD FACSCanto II flow cytometer with a 488 nm laser to excite GFP, and 10,000 total cells were counted for each sample. Fluorescence images were taken on a Zeiss Axiovert 40 CFL tabletop microscope with a 10  $\times$  Plan-A objective with a 50 W HBO lamp and blue filter cube for excitation. Images were captured with a Canon EOS RebelXS camera connected to the microscope.

## 3. Results and Discussion

### 3.1 Coating BT with PEI yields positively charged non-cytotoxic complexes

BT-PEI complexes prepared with different concentrations of PEI were characterized for their size and zeta potentials (Fig. 1). Complex sizes are unaffected by PEI concentration (Fig. 1A). Zeta potential of the complexes, on the other hand, becomes more positive with increasing PEI concentration due to the positively charged amine groups on the PEI (Fig. 1B). Since zeta potentials of complexes stabilize at 25  $\mu\text{g/ml}$  PEI, this concentration was chosen for subsequent experiments. Particle size readings indicate a single monodisperse population, suggesting lack of excess PEI. Thus, under these formulation conditions, the weight ratio of PEI to BT in the composite nanoparticle is approximately 1:40. This composition was verified with thermogravimetric analysis, which showed the weight composition due to the polymer to be 2.3%, corresponding to about a true weight ratio of 1:43. Lower PEI concentrations produce complexes that have a statistically significant difference in zeta potential compared to the value seen at 500  $\mu\text{g/ml}$  PEI. The positive zeta potential should aid in the cellular uptake of the complexes by mediating binding to the

negatively charged cell surfaces [19], as well as enable condensation of negatively charged nucleic acids.

The BT-PEI particles display minimal cytotoxicity in HeLa cells as evidenced by an MTT assay (Fig. 2). The concentration of particles tested in the cytotoxicity assay is 2.5-fold higher than in the following uptake and transfection studies, and both concentrations are at least 10-fold less than the reported LD50 of PEI; therefore, the BT-PEI complexes are not cytotoxic at the working concentrations used in this work. The components of the complex, either individually or together as a complex, do not decrease cell viability dramatically. The lack of cytotoxicity of PEI and BT-PEI particles is consistent with previous values of the LD50 of PEI (16 – 42  $\mu\text{g/ml}$  [20,21]).

### 3.2 Coating BT with PEI improves cellular uptake

PEI complexation increases the uptake of BT NPs into HeLa cells (Fig. 3). The BT particles were detected by taking advantage of their inherent second harmonic generating (SHG) signal, which has an optimal emission at 410 nm (Fig. 3A). BT NPs without any modifications are internalized into cells but at a much lower efficiency compared to the BT-PEI complexes. The PEI coating resulted in an 8-fold increase in the number of particles per cell (Fig. 3B), which would be beneficial for increased contrast enhancement for biomedical imaging. The SHG signal per cell increased about 20-fold for BT-PEI over BT alone, indicating a significant contrast enhancement due to enhanced cell uptake (Fig. S1). Additional optimization of BT-PEI dose and cell culture conditions should improve cellular uptake further. The particles, although too large to enter cells via endocytic mechanisms, may be able to be taken up by alternate uptake mechanisms, such as macropinocytosis [22].

The positive charge imparted by the PEI coating significantly increased the uptake of BT NPs into cells. Other types of NPs have been coated similarly with cationic polymers, resulting in increased cellular uptake [23,24]. While the BT NPs alone are able to enter cells, any application desiring a high signal to background ratio for diagnostic purposes requires as many signal generating particles as possible to enter the target cells. While the cellular uptake properties imparted by the PEI leads to nonspecific cell binding and endocytosis, this form of broad improvement in internalization may be advantageous for *ex vivo* gene delivery applications where target cells have already been isolated [25]. For example, isolated cells can be treated with BT-PEI carrying genes in an *ex vivo* transfection setting, the transfected cells loaded with the BT nanoprobe can be reintroduced into patients, and finally imaging can be used to track the location of the cells. Towards this end, we next tested the ability of BT-PEI complexes to deliver genes into cells.

### 3.3 BT-PEI complexes effectively deliver DNA

The BT-PEI complexes were tested for their ability to deliver DNA to cells. For this study, 25 ng of pGFP was added to BT-PEI and vortexed, resulting in slightly larger complexes (Fig. 4A). The polydispersity index (PDI) is equal to 1 for the BT-PEI/DNA sample, indicating a monodisperse population of particles. Both BT-PEI/DNA and PEI/DNA complexes display low transfection rates at low N/P ratios (Fig. 4B). Higher N/P ratios allow both PEI/DNA and BT-PEI/DNA complexes to be able to deliver genetic material into

cells efficiently (Fig. 4B and C) This data suggests that the presence of BT does not interfere with the ability of PEI to deliver genes into cells, and provides support towards the development of complexes with dual functions – agents that enable coupled imaging and gene transfection.

Future studies will be aimed at understanding the mechanism of gene delivery with the BT-PEI/DNA complexes. For example, it is presently unclear if and when the various components of the BT-PEI/DNA complex disassemble during the transfection process. The intracellular fate of the BT NPs, and whether the presence of PEI alters BT trafficking in cells, is also currently unknown. Furthermore, if higher stability complexes are desired for certain biomedical applications, cross-linking of the polymer component combined with environment-responsive release of cargo DNA can be engineered into the system [26].

#### 4. Conclusion

As a recently established class of NPs for biological imaging, BT may be ideal to use in particle tracking experiments [27–28] due to their lack of bleaching or blinking and overall safety. Here, we have significantly improved the cellular uptake of the BT NPs by coating them with PEI. Both the positive charge and low toxicity of PEI at the concentrations used make it a promising choice for creating BT-polymer complexes, especially in the context of developing multi-functional vectors capable of coupled imaging and nucleic acid delivery. The PEI component will enable effective gene delivery while the BT component will enable SHG imaging. While the emission signal spectrum of BT may be at wavelengths too short to be detectable across thick tissues, imaging in thin tissues or using endoscopically guided microscopes can take advantage of the strong, precise BT signal in the *in vivo* environment.

#### Supplementary Material

Refer to Web version on PubMed Central for supplementary material.

#### Acknowledgments

This project was supported by the Nanobiology Interdisciplinary Graduate Training Program of the W. M. Keck Center for Interdisciplinary Bioscience Training of the Gulf Coast Consortia (NIH Grant No. T32 EB009379) to C.D. We would like to thank Tegye Vadakkan in the Optical Imaging and Vital Microscopy (OIVM) core at the Baylor College of Medicine for assistance with SHG imaging.

#### References

1. Kurtz S. New nonlinear optical materials. *Quantum Electronics*. 1968; 4:578.
2. Pantazis P, Maloney J, Wu D, Fraser SE. Second harmonic generating nanoprobe for *in vivo* imaging. *PNAS*. 2010; 107:14535. [PubMed: 20668245]
3. Hsieh CL, Grange R, Pu Y, Psaltis D. Three-dimensional harmonic holographic microscopy using nanoparticles as probes for cell imaging. *Optics Express*. 2009; 17:2880. [PubMed: 19219192]
4. Masters, BR.; So, P., editors. *Handbook of biomedical nonlinear optical microscopy*. Vol. 1. Oxford, New York: 2008. Chapter 2.
5. Derfus AM, Chan WCW, Bhatia SN. Probing the cytotoxicity of semiconductor quantum dots. *Nano Lett*. 2000; 4:11.



6. Ciofani G, Danti S, D'Alessandro D, Moscato S, Petrini M, Menciassi A. Barium titanate nanoparticles: highly cytocompatible dispersions in glycol-chitosan and doxorubicin complexes for cancer therapy. *Nanoscale Res. Lett.* 2010; 5:1093. [PubMed: 20596329]
7. Ciofani G, Danti S, Moscato S, Albertazzi L, D'Alessandro D, Dinucci D, Chiellini F, Petrini M, Menciassi A. Preparation of stable dispersion of barium titanate nanoparticles: potential applications in biomedicine. *Coll. and Surf. B: Biointerfaces.* 2010; 76:535.
8. Akinc A, Langer R. Measuring the pH environment of DNA delivered using nonviral vectors: implications for lysosomal trafficking. *Biotech. and Bioeng.* 2001; 78:503. 78.
9. Boussif O, Lezoualc'h F, Zanta MA, Mergny MD, Scherman D, Demeneix B, Behr JP. A versatile vector for gene and oligonucleotide transfer into cells in culture and in vivo: polyethylenimine. *PNAS.* 1995; 92:7297. [PubMed: 7638184]
10. Kievit FM, Veiseh O, Bhattarai N, Fang C, Gunn JW, Lee D, Ellenbogen RG, Olson JM, Zhang M. PEI-PEG-chitosan-copolymer-coated iron oxide nanoparticles for safe gene delivery: synthesis, complexation, and transfection. *Adv. Funct. Mater.* 2009; 19:2244. [PubMed: 20160995]
11. Lee Y, Miyata K, Oba M, Ishii T, Fukushima S, Han M, Koyama H, Nishiyama N, Kataoka K. Charge-conversion ternary polyplex with endosome disruption moiety: a technique for efficient and safe gene delivery. *Ang. Chem.* 2008; 120:5241–5244.
12. Qi L, Gao X. Quantum dot-amphipol nano complex for intracellular delivery and real-time imaging of siRNA. *ACS Nano.* 2008; 7:1403. 7. [PubMed: 19206308]
13. Fuller JE, Zugates GT, Ferreira LS, Ow HS, Nguyen NN, Wiesner UB, Langer RS. Intracellular delivery of core-shell fluorescent silica nanoparticles. *Biomater.* 2008; 29:1526.
14. Xia T, Kovochich M, Liang M, Meng H, Kabehie S, George S, Zink J, Nel A. Polyethyleneimine coating enhances the cellular uptake of mesoporous silica nanoparticles and allows safe delivery of siRNA and DNA constructs. *ACS Nano.* 2009; 3:3273–3286. [PubMed: 19739605]
15. Leung K, Chak C, Lee S, Lai J, Zhu X, Want Y, Sham K, Cheng C. Enhanced cellular uptake and gene delivery of glioblastoma with deferoxamine-coated nanoparticle/plasmid DNA/branched polyethylenimine composites. *Chem. Comm.* 2013; 49:549–551. [PubMed: 23192002]
16. Benoit D, Zhu H, Lilierose M, Verm R, Ali N, Morrison A, Fortner J, Avendano C, Colvin V. Measuring the grafting density of nanoparticles in solution by analytical ultracentrifugation and total organic carbon analysis. *Anal. Chem.* 2012; 84:9238–9245. [PubMed: 22967239]
17. Marti O, Holzwarth M, Beil M. Measuring the nanomechanical properties of cancer cells by digital pulsed force mode imaging. *Nanotech.* 2008; 19:1–7.
18. Theer P, Hasan M, Denk W. Two-photon imaging to a depth of 1000  $\mu\text{m}$  in living brains by use of a Ti:Al<sub>2</sub>O<sub>3</sub> regenerative amplifier. *Opt. Lett.* 2003; 28:1022–1024. [PubMed: 12836766]
19. He C, Hu Y, Yin L, Tang C, Yin C. Effects of particle size and surface charge on cellular uptake and biodistribution of polymeric nanoparticles. *Biomater.* 2010; 31:3657.
20. Wang J, Zhang PC, Lu HF, Ma N, Wang S, Mao H, Long KW. New polyphosphoramidate with a spermidine side chain as a gene carrier. *J. Cont. Rel.* 2002; 83:157.
21. Xu F, Chai M, Li W, Ping Y, Tang G, Yang W, Ma J, Liu F. Well-defined poly(2-hydroxyl-3-(2-hydroxyethylamino)propyl methacrylate) vectors with low toxicity and high gene transfection efficiency. *Biomacromol.* 2010; 11:1437–1442.
22. Dausend J, Musyanovych A, Dass M, Walther P, Schrezenmeier H, Landfester K, Mailander V. Uptake mechanism of oppositely charged fluorescent nanoparticles in HeLa cells. *Macromol. Biosci.* 2008; 8:1135–1143. [PubMed: 18698581]
23. Babic M, Horak D, Trchova M, Jendelova P, Glogarova K, Lesny P, Herynek V, Hajek M, Sykova E. Poly(L-lysine)-modified iron oxide nanoparticles for stem cell labeling. *Bioconj. Chem.* 2008; 19:740.
24. Petri-Fink A, Steitz B, Finka A, Salaklang J, Hofmann H. Effect of cell media on polymer coated superparamagnetic iron oxide nanoparticles (SPIONs): colloidal stability, cytotoxicity, and cellular uptake studies. *EJPB.* 2008; 68:129.
25. Davda J, Labhasetwar V. Characterization of nanoparticle uptake by endothelial cells. *Int. J. Pharm.* 2002; 233:51. [PubMed: 11897410]
26. Kang Y, Taton TA. Controlling shell thickness in core-shell gold nanoparticles via surface-templates adsorption of block copolymer surfactants. *Macromol.* 2005; 38:6115.

27. Huang F, Dempsey C, Chona D, Suh J. Quantitative nanoparticle tracking: applications to nanomedicine. *Nanomed.* 2011; 6:693.
28. Suh J, Wirtz D, Hanes J. Efficient active transport of gene nanocarriers to the cell nucleus. *PNAS.* 2003; 100:3878. [PubMed: 12644705]

Author Manuscript

Author Manuscript

Author Manuscript

Author Manuscript



### Highlights

- Barium titanate nanoparticles were complexed with linear polyethylenimine
- BT-PEI complexes entered cells eight-fold better than BT alone
- Second harmonic generation imaging was used to image BT-PEI complexes
- BT-PEI can deliver DNA to cells efficiently

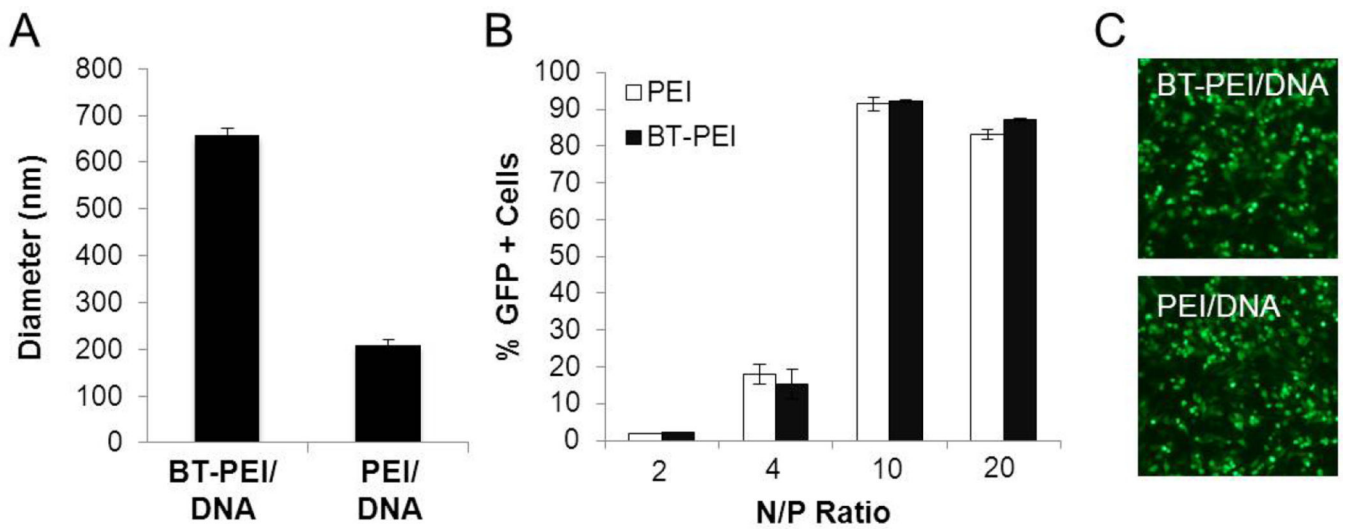


**Figure 1. PEI adsorption to BT alters nanoparticle properties**

(A) Hydrodynamic diameter of BT-PEI complexes formed with different PEI concentrations. ANOVA shows no statistical difference between populations. (B) Zeta potential of BT-PEI complexes formed with different PEI concentrations. \* $p < 0.05$ , \*\* $p < 0.01$  (student's t test)

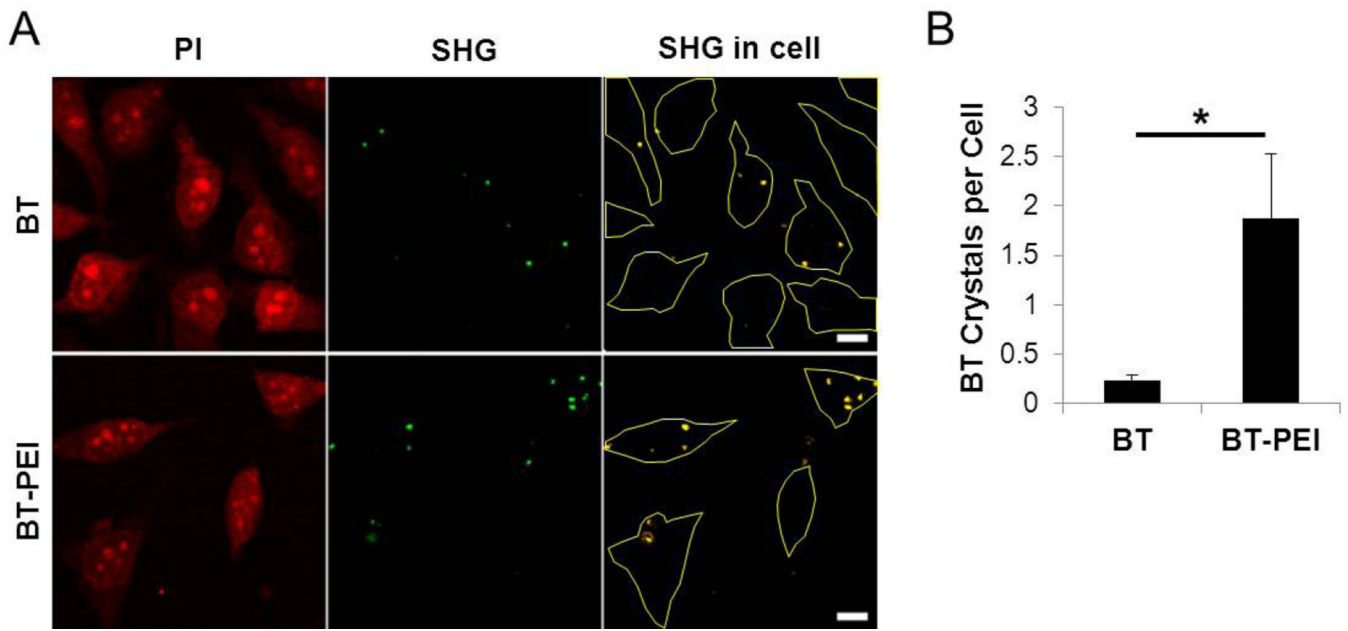


**Figure 2. BT-PEI is not cytotoxic**

Cells were exposed to BT-PEI, BT, PEI, or buffer only and incubated for 24 hours prior to performing an MTT assay for viability. One-way ANOVA shows no statistical difference between populations.

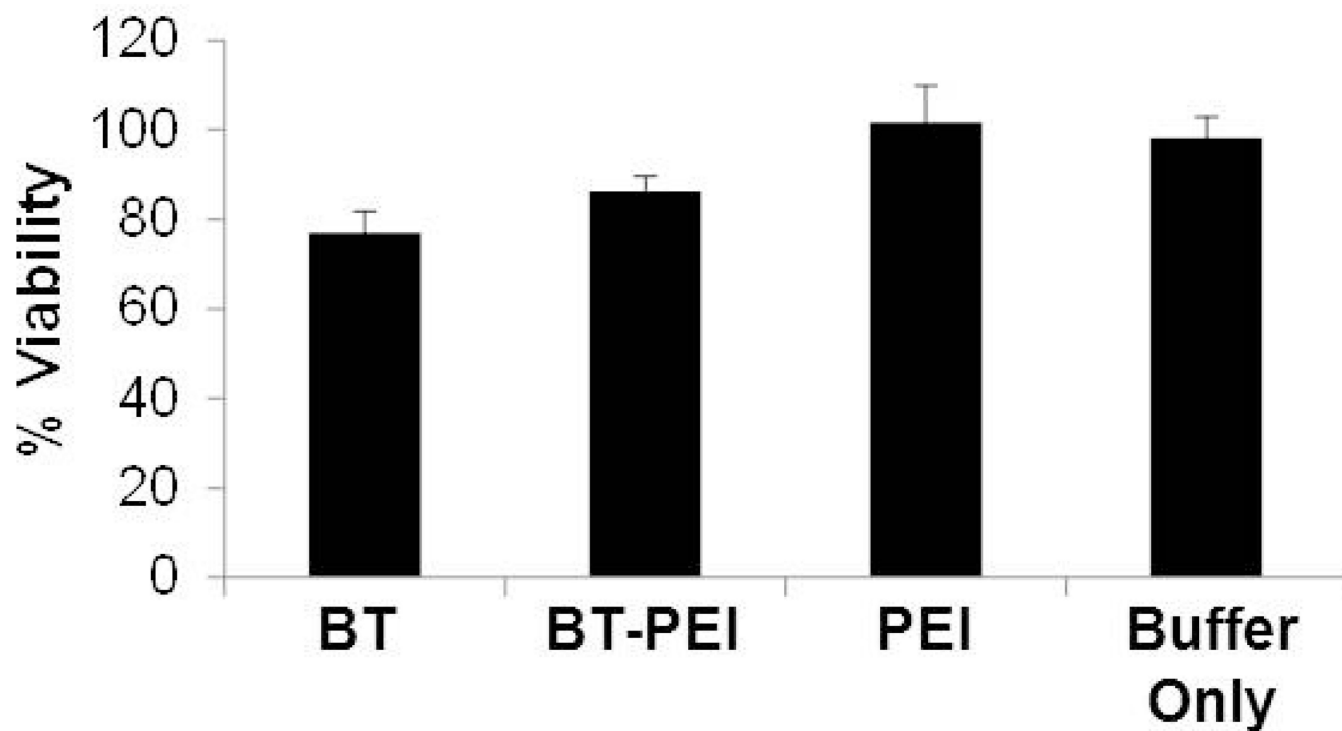


**Figure 3. PEI coating enhances cellular uptake of BT**

(A) BT or BT-PEI at a weight ratio of polymer to NP of 1:40 were added to HeLa cells and incubated for 3 hours prior to fixing and propidium iodide (PI) staining. PI signal allows for discernment of cell boundaries and SHG indicates the signal from the BT particles.

Colocalization between these two channels is shown in the rightmost panel to identify internalized particles. Cell outlines are shown in yellow. (B) BT or BT-PEI particles were counted in 4 different fields of view each to determine an average number of internalized NPs per cell. \*  $p < 0.01$  (student's t test). Scale bars represent 10  $\mu\text{m}$ .

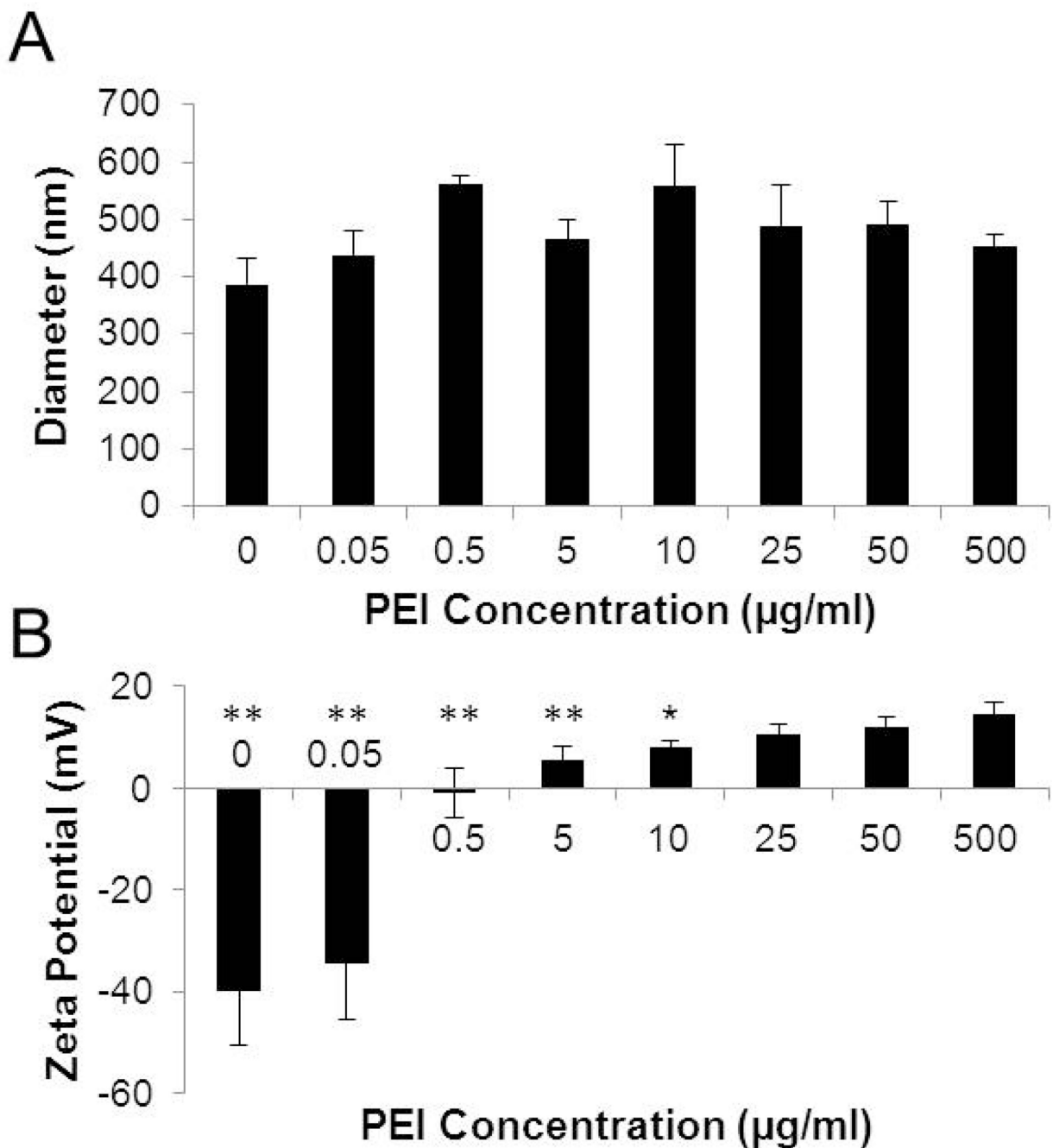


**Figure 4. BT-PEI complexes can deliver DNA effectively**

(A) Complex size with condensed DNA. Polydispersity index (PDI) is indicated for each sample. (B) Flow cytometry transfection data for BT-PEI/DNA or PEI/DNA complexes formed at various N/P ratios. (C) Fluorescence micrographs of cells transfected with BT-PEI/DNA or PEI/DNA (both at N/P = 10 carrying pGFP) at 24 hours post transfection.